Metasurface Absorber-Based Circularly Polarized Antenna for 5G mmWave Applications

Abdul Majeed, Yejun He* and Shahid Ullah
State Key Laboratory of Radio Frequency Heterogeneous Integration
Sino-British Antennas and Propagation Joint Laboratory of MOST
Guangdong Engineering Research Center of Base Station Antennas and Propagation
Shenzhen Key Laboratory of Antennas and Propagation
College of Electronics and Information Engineering, Shenzhen University, 518060, China
Email: heyejun@126.com*

***Abstract*—This paper describes a metasurface (MS) absorber-based circularly polarized (CP) antenna for 5G mmWave applications. A simple circular notched edge antenna with rectangular slot and ″+″-shaped slot on the ground plane operating at the fundamental mode of the desired frequency band is utilized. Additionally, rectangular patch-based MS is designed to operate at the same fundamental mode as the antenna, and the MS is positioned above the antenna at a specified distance to achieve the desired 3-dB axial ratio bandwidth (ARBW) and a 2.2-dBi gain enhancement while maintaining an appropriate size of 30 $\times$ 36 $\times$ 0.254 mm^3. The antenna achieved impedance bandwidth ($|S_{11}| \leq -$ 10 dB) without MS from 27.18 GHz up to 28.63 GHz and realized a gain of around 4.8 dBi at 28 GHz. The antenna with MS achieved an impedance bandwidth (IBW) from 27.00 GHz up to 29.20 GHz and realized a gain of around 7.0 dB at 28 GHz, and radiation efficiency above of 80%. The proposed antenna is a potential candidate for upcoming 5G applications.**

***Index Terms*—circularly polarized, 5G mmWave, metasurface, axial ratio, gain.**

I. Introduction

The development of mobile communication technology is the latest revolution in the mobile industry [1]. The requirement for reliable connectivity, faster data rates, more bandwidth, and greater user capacity is driving the advancement of mobile technology [2]. To keep up with the growing bandwidth and data rates, a new technology known as fifth generation (5G) was created [3]. Two widely-used frequency bands have been allocated for 5G technologies, following extensive research and analysis. There are two frequency bands: the lower band, or sub-6 GHz, and the higher band, or millimeter waves. Since the 6 GHz range (3-6 GHz) is currently congested with applications, it is necessary to build actual mmWave communication with unlicensed and unrestricted bandwidth [4], [5]. Frequencies in the mmWave range, such as 28 GHz and 38 GHz, have been identified as potential candidates for future 5G standards [6], [7].

By applying a greater portion of the spectrum, faster data rates and bandwidth can be attained. But atmospheric attenuation such as rain, fog, and snow affects these frequencies. By utilizing antennas with high gain and directivity, these atmosphere attenuation challenges can be overcome. A few techniques for improving an antenna's gain and directivity are using an antenna array [8], [9], adding an artificial magnetic conductor (AMC) underneath the antenna [10], [11], and using the FSS. These methods can be applied to mmWave and microwave antenna gain enhancement [12]. An antenna gain of 5.5 dBi is achieved by introducing and presenting a 33 GHz bowtie-slotted antenna with AMC [10]. The AMC-based patch antenna operating at 28 GHz with a gain of 4.77 dBi is covered in [11].

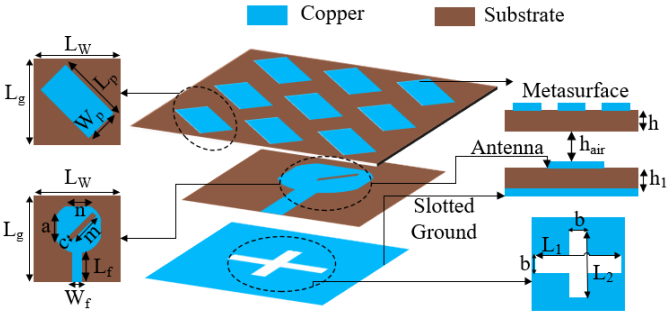

Fig. 1. Depolyed view of the proposed antenna with metasurface superstrate.

This work proposes adding a 28 GHz CP antenna to the MS absorber in order to increase the antenna gain. The proposed antenna has been designed specifically for new 5G applications. An MS-based absorber placed atop the antenna increases the ARBW(AR $\leq$ 3 dB) and gain(dBi) by approximately 7 dB. The antenna with MS obtained good impedance bandwidth (IBW) in the mmWave frequency range. In summary, the proposed antenna exhibits a compact design, appropriate gain, and ease of use in the feeding network.

II. Metasurface-Based CP Antenna Design

The perspective view of the proposed single antenna with dimensions of 10 mm $\times$ 12 mm $\times$ 0.787 mm based on the MS superstrate is illustrated in Fig. 1. The circular notched edge single antenna with rectangular slot is placed on a Rogers RT5880 substrate with a dielectric constant and thickness (h_1) of 2.2 and 0.787 mm, respectively. A simple ″+″-shaped slot is etched from a ground plane on the other side of the substrate. An array of 3 $\times$ 3 MS with dimensions of 30 mm $\times$ 36 mm is printed on same substrate (thickness h = 0.254 mm) and

ICC 2025 - IEEE International Conference on Communications | 979-8-3315-0521-9/25/$31.00 ©2025 IEEE | DOI: 10.1109/ICC52391.2025.11161208

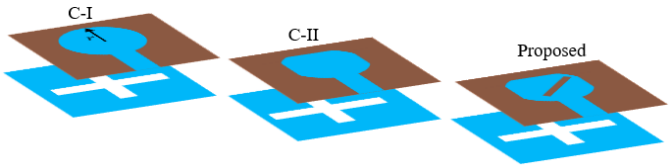

Fig. 2. Evaluation steps of the proposed antenna (a) C-I (b) C-II and (c) proposed.

TABLE I
DIMENSIONS OF THE PROPOSED ANTENNA

Parameters	Values (mm)	Parameters	Values (mm)	Parameters	Values (mm)
Lw	10	Lg	12	Wp	3.2
Lp	9.0	Lf	4.0	Wf	2.4
L_1	4.0	L_2	3.0	m	4.0
n	3.39	b	0.4	a	2.15
c	0.4	r	3.0	–	–

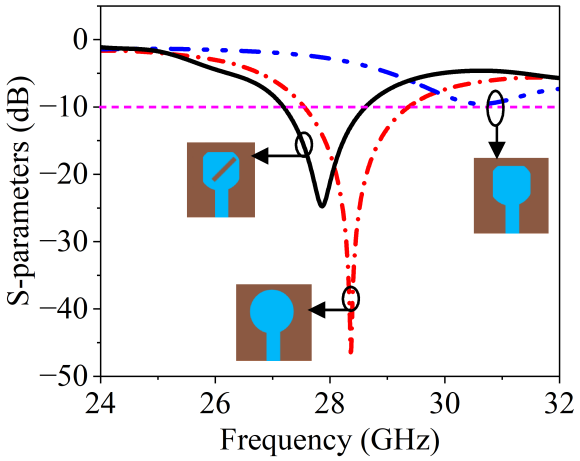

Fig. 3. Simulated results of stepwise design: C-I, C-II and proposed.

placed on the top of the single antenna at height of 4.2 mm (h_{air}). The other optimized parameters of the antenna and MS are tabulated in Table I.

A. Single Antenna Element Design and CP conversion

This section discusses the single antenna design and linear to circular polarization conversion procedures. Fig. 2 shows the stepwise design cases. In case 1, a circular radiator by a 50 Ω microstrip feed line with a $''+''$-shaped slot on the ground plane was first introduced (denoted by C-I). A small rectangular open slot was top-loaded into the circular radiator in case 2 (C-II) and edge-sided. Finally, a 45° rectangular slot was inserted into circular radiator to achieve CP performance in step 3 (proposed). Fig. 3 shows that C-I achieves the impedance matching below 10 dB throughout the bandwidth of (27.55–29.35 GHz) at resonance frequency 28.36 GHz. As Fig. 3 shows, C-II provides poor impedance matching at the resonance frequency of 30.61 GHz and is not an antenna. Nonetheless, the proposed single antenna achieves good impedance matching at the resonance frequency of 27.87

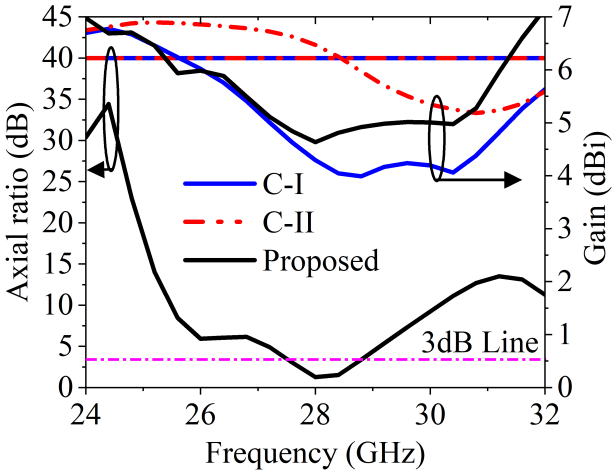

Fig. 4. Simulated results of axial ratio (AR $\leq$ 3dB) and gain(dBi) of stepwise design.

GHz with 10 dB IBW of 27.17–28.63 GHz, respectively, as shown in Fig.3. The axial ratio and gain (dBi) of the stepwise design are shown in Fig. 4. Nevertheless, as shown in Fig. 4, the first two steps (C-I and C-II) demonstrate that the gain is above 4 and 5 dBi, and the axial ratio (AR$\leq$ 3 dB) values are 40 dB, indicating no CP performance. The proposed antenna has a fully overlapping 3.9% axial ratio bandwidth (27.60 – 28.72 GHz) with a gain of 4.8 dBi, as illustrated in Fig. 4.

B. Absorber Structure with Equivalent Circuit

The absorber unit cell with an equivalent circuit is displayed in Fig. 5. The dimensions of the MS unit cell are 10 mm $\times$ 12 mm. The equivalent circuit has the following components: C_1 = 0.11 pF and L_1 = 0.294 nH for the inductance. The CST 2022 software simulates the metasurface absorber using the unit cell boundary conditions in the x- and y-direction. For excitation, the Floquet ports are used in the $\pm z$-direction. The equivalent circuit model of the absorber unit cell is designed and executed using the Keysight's advanced design system (ADS) simulation tool. Meanwhile, the bottom of the substrate lacks any copper or other conductor material to allow the electromagnetic current from the antenna to pass through to the superstrate. Fig. 5 displays the reflectivity and absorptivity results of the equivalent circuit and CST software. The absorptivity of proposed MS is calculated by A = 1-$|S_{11}|^2$-$|S_{21}|^2$. The reflectivity and transmissivity of MS absorber to frequency are denoted by $|S_{11}|^2$ and $|S_{21}|^2$, respectively. According to Fig. 5, the reflectivity and absorptivity results using an ADS circuit and CST simulation demonstrate that the MS absorber absorbs more than 90% of electromagnetic waves in the frequency ranges of 27.18–28.72 GHz. Additionally, reflectivity tends to zero in these frequency ranges. Fig. 5 compares the reflectivity and absorptivity results by circuit simulators (ADS) and ADS, and results demonstrate a good agreement.

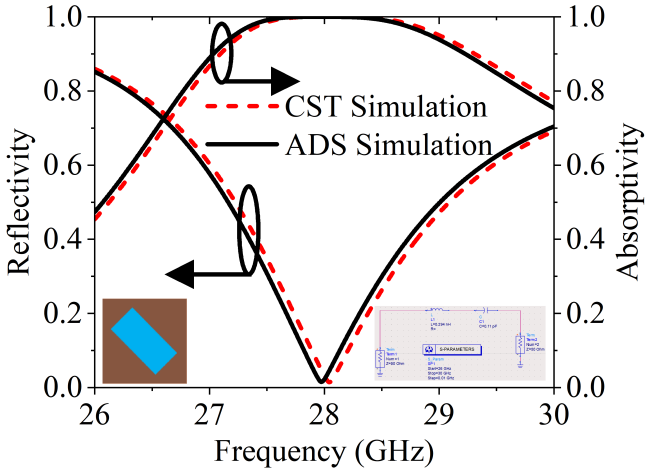

Fig. 5. Simulated results of absorptivity and reflectivity.

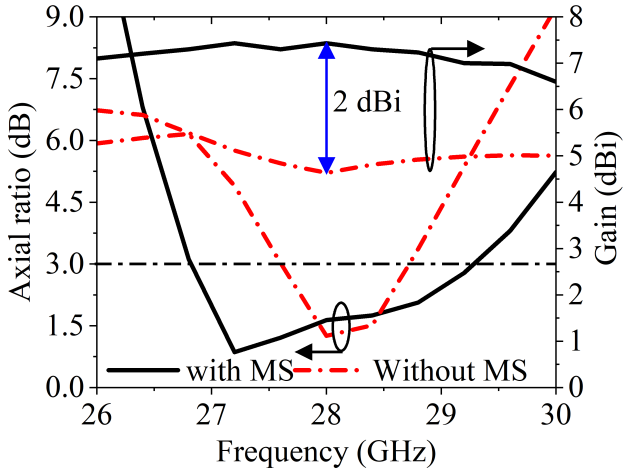

Fig. 7. Axial ratio (AR $\leq$ 3dB) and gain (dBi) with and w/o metasurface.

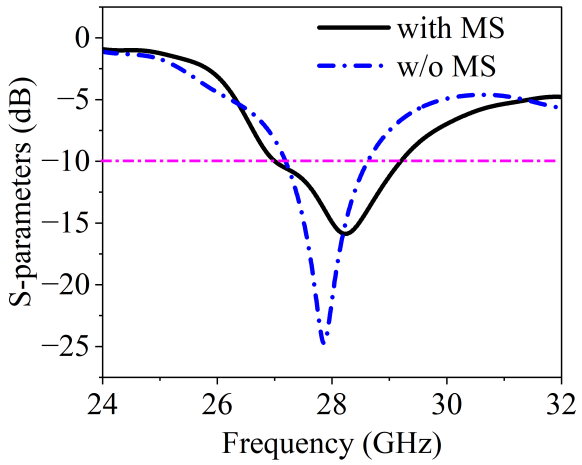

Fig. 6. S-parameters with and without metasurface.

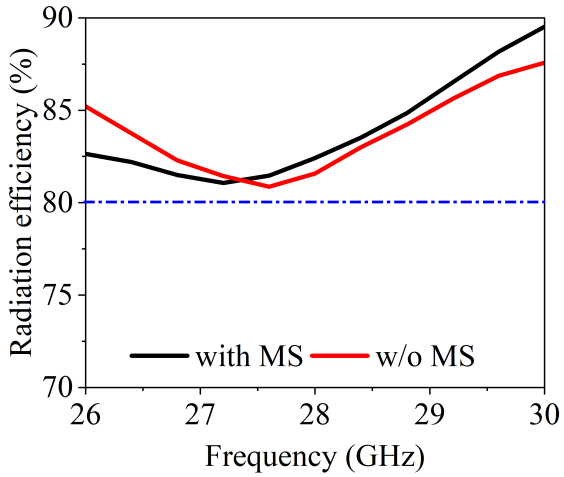

Fig. 8. Simulated result of radiation efficiency (%) with and w/o metasurface.

C. Gain Enhancement

This section introduces a single antenna concept to increase the antenna gain. Fig. 6 shows the impedance matching of the proposed single antenna with and without (w/o) MS absorber. Fig. 6 displays the simulated results of IBW ($|S_{11}| \leq -10$ dB) with and w/o metasurface from 27.00–29.20 GHz (2.2 GHz) and 27.18–28.63 GHz (1.45 GHz), respectively. Fig.6 shows that the impedance bandwidth is enhanced by 0.75 GHz due to MS. Fig. 7 shows the gain (dBi) of the proposed antenna with and w/o metasurface at 28 GHz. The gain and ARBW of antenna w/o metasurface is 4.8 dBi and 3.9% (27.60 – 28.72 GHz). The addition of metasurface increases system gain and ARBW by improving the gain and ARBW of the proposed antenna. Therefore, the metasurface absorber-based antenna provides a high gain of up to 7 dBi at 28 GHz, which was 4.8 dBi w/o metasurface and increases the ARBW of 8.8% (26.81–29.28 GHz), as illustrated in Fig. 7. In addition, Fig. 8 shows the radiation efficiency with and w/o MS. As shown in Fig. 8, the radiation efficiency is greater than 80% in both cases with and w/o MS. Thus, Table II summarizes the performance of the proposed antenna with published work.

TABLE II
COMPARISON OF THE PROPOSED ANTENNA WITH PREVIOUS WORK

Ref.	IBW(GHz)	Gain(dBi)	Polarization	Size (mm^3)
[10]	32–34.60	5.5	LP	30×16×0.8
[11]	29.25–30.35	4.77	CP	23.85×44.9×1.52
[12]	27.3–28.20	5.0	LP	140×70×10
This work	27.00–29.20	7.0	CP	30×36×5

III. Conclusion

The gain and ARBW of the single antenna for 5G networks are improved based on metasurface absorber. The MS with 3 × 3 cells is used to achieve the required gain enhancement. The overlapping of the simulated 10 dB IBW and 3 dB ARBW

shows good impedance matching and CP performance. The antenna gain is enhanced by 2.2 dBi and 4.9% ARBW at an operating frequency of 28 GHz. The proposed antenna has strong potential applications in the upcoming 5G networks.

ACKNOWLEDGMENT

This work is supported by National Key Research and Development Program of China under Grant 2023YFE0107900, in part by the National Natural Science Foundation of China under Grant 62071306, and in part by Shenzhen Science and Technology Program under Grants JCYJ20241202124219023, JCYJ20200109113601723 and JSGG20210420091805014.

REFERENCES

[1] M. Abirami, "A review of patch antenna design for 5G," in *Proc. IEEE Int. Conf. Electr., Instrum. Commun. Eng.* (ICEICE), pp. 1-3, Apr. 2017.

[2] J. Zhang, X. Yu, and K. B. Letaief, "Hybrid beamforming for 5G and beyond millimeter-wave systems: A holistic view," *IEEE Open J. Commun. Soc.*, vol. 1, pp. 77-99, 2020.

[3] S.-J. Park, D.-H. Shin, and S.-O. Park, "Low side-lobe substrate-integrated-waveguide antenna array using broadband unequal feeding network for millimeter-wave handset device," *IEEE Trans. Antennas Propag.*, vol. 64, no. 3, pp. 923-932, Mar. 2016.

[4] A. Khan, Y. He and Z. N. Chen, "A Dual-Band Quad-Port Circularly Polarized MIMO Antenna Based on a Modified Jerusalem-Cross Absorber for Wireless Communication Systems," *IEEE Trans. Antennas Propag.*, vol. 72, no. 1, pp. 310-322, Jan. 2024.

[5] Q. Zhu, K. Bo Ng, C. Hou Chan, and K.-M. Luk, "Substrate-integrated-waveguide-fed array antenna covering 5771 GHz band for 5G applications," *IEEE Trans. Antennas Propag.*, vol. 65, no. 12, pp. 6298-6306, Dec. 2017.

[6] R. Przesmycki, M. Bugaj, and L. Nowosielski, "Broadband microstrip antenna for 5G wireless systems operating at 28 GHz," *Electronics*, vol. 10, no. 1, p. 1, Dec. 2020.

[7] Z. Ye, T. Ding, Y. Liu, P. Chen, J. Xiao and Q. Ye, "A Millimeter-Wave Circularly Polarized Antenna," in *Proc. 2022 Cross Strait Radio Science & Wireless Technology Conference (CSRSWTC)*, pp. 1-2, 2022.

[8] J. A. Nasir, M. U. Rehman, A. J. Hashmi, and W. T. Khan, "A compact low cost high isolation substrate integrated waveguide fed slot antenna array at 28 GHz employing beamforming and beam scanning for 5G applications," in *Proc. 12th European Conference on Antennas and Propagation (EuCAP 2018)*, London, U.K., pp. 1-5, 2018.

[9] S. X. Ta, H. Choo, and I. Park, "Broadband printed-dipole antenna and its arrays for 5G applications," *IEEE Antennas Wireless Propag. Lett.*, vol. 16, pp. 2183-2186, 2017.

[10] A. A. Althuwayb, "MTM-and SIW-inspired bowtie antenna loaded with AMC for 5G mm-wave applications," *Int. J. Antennas Propag.*, vol. 21, Jan. 2021, Art. no. 6658819.

[11] M. A. So, K. Saurav and S. K. Koul, "Four-Port Orthogonal Circularly Polarized Dual-Band MIMO Antenna With Polarization and Spatial Diversity Using a Dual-Band Linear-to-Circular Polarization Converter," *IEEE Trans. Antennas Propag.*, vol. 70, no. 9, pp. 8554-8559, Sep. 2022.

[12] H. Li, Y. Cheng, L. Mei and F. Wu, "Dual-Polarized Frame-Integrated Slot Arrays for 5G Mobile Handsets," *IEEE Antenna Wirel. Propag. Letts.*, vol. 9, no. 11 pp. 1953-1957, Jul. 2024.